

Evaluation of corrosion and wear resistance titanium nitride (TiN) coated on mild steel (MS) with brush plated nickel interlayer

B. Subramanian^{*1}, K. Ashok¹, K. Subramanian², D. Sastikumar³, G. Selvan⁴ and M. Jayachandran¹

Titanium nitride (TiN) coatings were deposited on mild steel (MS) by direct current reactive magnetron sputtering. With the aim of improving the corrosion resistance of TiN, an additional nickel interlayer was brush plated on the steel substrates before TiN film formation. The phases have been identified with X-ray diffraction analysis. The hardness values of TiN layers were found to increase with the increase in thickness of the Ni interlayer. The wear track investigations of TiN layers showed that the TiN/MS system was worn out by abrasive wear mechanism while on the film with Ni interlayer is by adhesive wear. It was found that the TiN/Ni/MS stack had a weaker tendency towards corrosion and higher corrosion resistance in 3.5%NaCl than the bare MS substrate, Ni/MS and TiN/MS specimen.

Keywords: Titanium nitride, Magnetron sputtering, Hard coatings, Corrosion resistance

Introduction

Titanium nitride (TiN) has an excellent combination of hardware performance properties, aesthetic appearance and contamination safety (surgical tools and implants, as well as food contact applications). TiN coatings are widely employed in semiconductor manufacturing industry as a 'diffusion barrier' layer,^{1,2} gate electrodes in field effect transistors, and in very large scale integrated microelectronics. In addition, metal nitrides are extremely suitable for manufacturing diverse miniaturised devices for thin film resistor,^{3,4} microelectronic mechanical systems,^{5,6} and in biotechnology.⁷ Generally, techniques like physical vapour deposition (PVD),⁸⁻¹⁰ plasma assisted chemical vapour deposition, plasma enhanced chemical vapour deposition and hollow cathodic ionic plating¹¹ are used in developing hard coatings on various substrates. The disadvantage of physical vapour deposited TiN coatings is that they inherently possess columnar microstructures leading to a large number of pores in the coatings.¹² The columnar structure allows the pores to run across the coating thickness so that the corrosive medium may attack the coating/substrate intersurface.¹³ It is, therefore, important to reduce the porosity of the hard coatings deposited on a substrate whose surface should be protected from corrosive attack. To improve the corrosion resistance of a substrate, PVD coatings of

TiN are used with a metallic interlayer, which acts as a protective barrier layer between the substrate and the corrosive medium present inside the pores and defects of TiN overlayer.¹⁴

TiN coatings sometimes have a greater tendency to failure, especially when coated on softer substrates. One reason is that the softer substrate could not provide effective support and strength for the TiN coating. Another is its poor adhesion to the substrate due to the different surface topography and morphological properties between the coating and the substrate. Therefore, the applications for these coatings are limited. To improve the adhesion and wear resistance, a composite coating with an interlayer, with suitable hardness, composition and adhesion strength, has been obtained.¹⁵ An electro less nickel interlayer was employed in TiN films deposited onto low carbon steel and an increase in both surface hardness and adhesion strength in the as derived TiN/Ni₃P/Fe coating stack was observed.¹⁶ The formation of an interface diffusion layer and a duplex composite layer at the interface enhanced the adhesion strength and hardness of the TiN composite coating.¹⁷

The aim of the present work is to study the mechanical properties and corrosion resistance of TiN thin film and with brush plated Ni interlayer on mild steel (MS) substrate deposited by reactive direct current (DC) magnetron sputtering.

Experimental

The substrate used was MS, consisting of 0.37C-0.28Si-0.66Mn-98.69Fe (wt-%). Coupons of the substrate were cut to a size of 75 × 25 mm and the surface was ground with SiC paper to remove the oxides and other contamination. The polished substrates were degreased with acetone and then cathodically electro cleaned in

¹ECMS Division, Central Electrochemical Research Institute, Karaikudi 630006, India

²Department of Mechanical Engineering, A.C. College of Engineering and Technology, Karaikudi 630006, India

³Department of Physics, National Institute of Technology, Trichy 620015, India

⁴Department of Physics, Thanthai Hans Rover College, Perambalur – 621212, India

*Corresponding author, email subramanianb3@gmail.com

alkali solution containing sodium hydroxide and sodium carbonate for 2 min at 70°C, followed by rinsing with triple distilled water. These substrates were subsequently dipped in 5 vol.-%H₂SO₄ solution for 1 min and thoroughly rinsed in distilled water.

A microprocessor controlled Selectron Power Pack Model 150 A-40 V (USA) was used to transform alternating current (AC) to DC in the brush plating set-up. The schematic of the brush plating system is given elsewhere.¹⁸ The DC power pack has two leads, one is the anode connected to the plating tool and the other is the cathode connected to the workpiece over which the coating has to be plated. The anode is covered with a porous absorbant material, which acts as the brush holding the solution. This wet brush can be moved on the surface of the workpiece that is to be finished (coated). When the anode touches the work surface the electrical circuit is formed and deposit is produced. The nickel electrolyte bath, similar to Watt's bath, contained 240 g L⁻¹ nickel sulphate, 40 g L⁻¹ nickel chloride and 30 g L⁻¹ boric acid. The pH and temperature were maintained at 4.0 and 28°C (room temperature) respectively. The optimised parameters used for the Ni brush plating are given in Table 1.

The layers of TiN were deposited on well cleaned MS substrates and brush plated Ni/MS specimen using a DC magnetron sputter deposition unit HIND HIVAC. The base vacuum of the chamber was below 10⁻⁶ Torr (1.33 × 10⁻⁴ Pa) and the substrate temperature was varied between 200 and 500°C. High purity argon was fed into the vacuum chamber for the plasma generation. The substrates were etched for 5 min at a DC power of 50 W and an argon pressure of 10 mTorr (1.33 Pa). A high purity (>99.999%) Ti target of 7.5 cm diameter was used as cathode. The deposition parameters for TiN sputtering are summarised in Table 2.

X-ray diffraction (XRD) was used to examine the changes in preferred grain orientation. X-ray diffraction patterns were recorded using an X'pert pro diffractometer using Cu K_α (1.541 Å) radiation from 40 kV X-ray source running at 30 mA. The surface of the coating was characterised by scanning electron microscopy (SEM) using a Hitachi S 3000H microscope and a molecular imaging atomic force microscope. Microhardness of the films on steel was evaluated using a DM-400 microhardness tester from LECO with Vickers indenters. A dwelling time of 15 s and a load of 25 and 5 g were used for the measurement.

Wear tests were carried out in a block on ring system. All tests were carried out at room temperature, ambient humidity and without lubrication. Steel ball bearing was used as a counter body. The ring material having the diameter of 60 mm was made of high chromium high carbon tool steel with Vickers hardness 850 HV. The load

applied on a specimen was 400 g (3.924 N) with the sliding speed of 100 rev min⁻¹. The wear rate was calculated by measuring the weight change of a specimen before and after the test. A conventional scratch tester (DUCOM TR-101 M4 scratch tester) was used to determine the scratch resistance of the coated layers on the substrate. The radius of the diamond pin was 0.2 mm. The load applied on a specimen was increased from the initial 2 N to the final 100 N with the loading rate of 5 N mm⁻¹ and the loading velocity of 0.2 mm s⁻¹.

Electrochemical polarisation studies were carried out using a BAS IM6 electrochemical analyser. Experiments were conducted using a standard three electrode configuration, with a platinum foil as the counter electrode, a saturated calomel electrode (SCE) as the reference electrode and the sample as the working electrode. The specimen (1.0 cm² exposed area) was immersed in the test solution of 3.5%NaCl. Experiments were carried out at room temperature (28°C). To establish the open circuit potential (OCP), before measurements the sample was immersed in the solution for ~60 min. Impedance measurements were conducted using a frequency response analyser. The spectrum was recorded in the frequency range of 10 mHz–100 kHz. The applied alternating potential had root mean square amplitude of 10 mV on the OCP. After reaching the stable OCP, the upper and lower potential limits of linear sweep voltammetry were set at ±200 mV with respect to OCP and the sweep rate was 1 mV s⁻¹. The Tafel plots were obtained after the electrochemical measurements. The porosity *P* was determined from the polarisation resistance and corrosion potential deduced from the potentiodynamic polarisation technique using the relation¹⁹

$$P = (R_{ps}/R_p) \times 10 - |\Delta E_{corr}|/b_a \quad (1)$$

where *R*_{ps} is the polarisation resistance of the MS substrate, *R*_p is the polarisation resistance of the coating, Δ*E*_{corr} is the difference between the corrosion potentials of the coating and the bare MS substrate and *b*_a is the anodic Tafel slope of the substrate.

Results and discussion

Structural and morphological properties

The XRD patterns of DC magnetron sputtered 2 μm thick TiN thin films deposited at various substrate temperatures *T*_s are shown in Fig. 1. The *d* spacing values match with JCPDS card no: 38-1420 for TiN thin film. Only a single phase TiN structure with fcc and the peaks corresponding to (111) and (200) planes are observed at 2θ=36.4 and 42.2°. The pattern reveals that (111) plane is the predominant crystallographic texture.

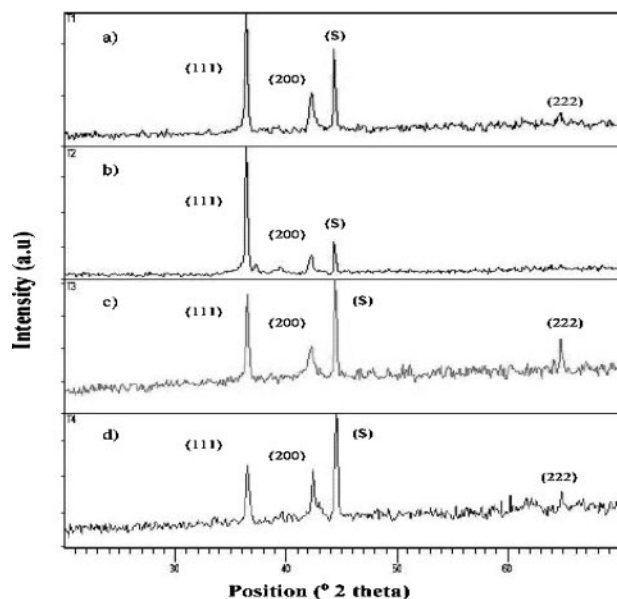
X-ray diffraction patterns of TiN coatings with Ni interlayer on MS substrates at different substrate temperatures *T*_s are shown in Fig. 2. The patterns show

Table 1 Optimised parameters for Ni brush plating

Objects	Specifications
Substrate	MS
NiSO ₄ , g L ⁻¹	240
NiCl ₂ , g L ⁻¹	40
Boric acid, g L ⁻¹	30
2-Butyl-1,4-diol, g L ⁻¹	1
Saccharine, g L ⁻¹	1.5
Sodium lauryl sulphate, g L ⁻¹	0.125
Bath temperature, °C	28
Anode	Graphite

Table 2 Deposition parameters for TiN reactive sputtering

Objects	Specifications
Target	Ti (99.9%)
Substrate	MS
Target to substrate distance, mm	60
Ultimate vacuum, Pa	1.33 × 10 ⁻⁴
Operating vacuum, Pa	0.2
Sputtering gas (Ar/N ₂)	1:1
Power, Watt	250
Substrate temperature, °C	400

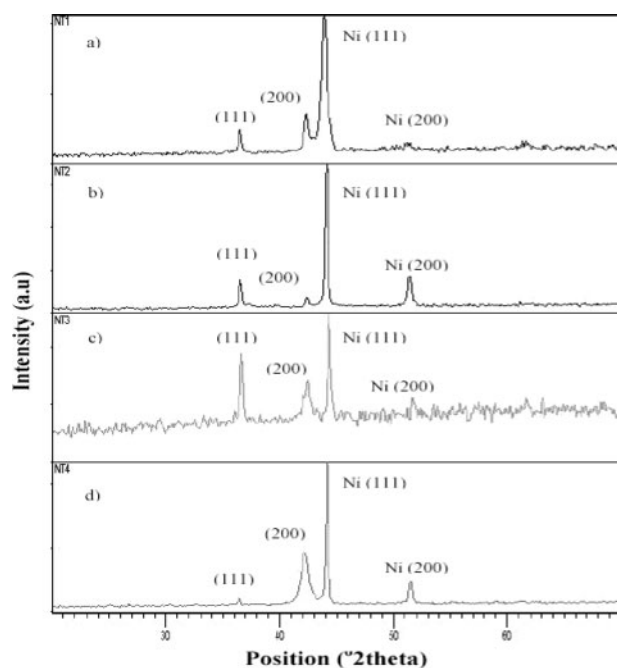


a 200°C; b 300°C; c 400°C; d 500°C

1 X-ray diffraction pattern for TiN at different substrate temperatures

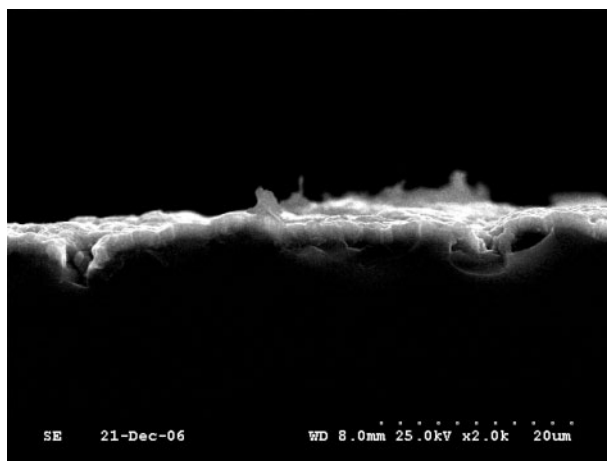
the predominant peaks for fcc Ni (JCPDS card no: 04-0850) interlayer along (111) and (200) planes in addition to that peaks identified for TiN along (111) and (200) planes at $2\theta=36.4$ and 42.3° . A constant thickness of $\sim 5 \mu\text{m}$ Ni interlayer was maintained for all the samples. Up to 400°C the peak intensity of TiN (111) plane increases and the intensity of (200) was found to increase at 500°C . Therefore the substrate temperature of 400°C was optimised for the deposition of TiN.

The cross-sectional and plane SEM photographs of TiN film on MS deposited at optimised condition are shown in Fig. 3. It is evident that the TiN films have a columnar structure (Fig. 3) with voids and boundaries throughout the film thickness. This growth process is



a 200°C; b 300°C; c 400°C; d 500°C

2 X-ray diffraction pattern for TiN with Ni interlayer at different substrate temperatures



3 Cross-sectional view of titanium nitride thin film

similar to that reported in the literature for TiN films.²⁰ This morphological study is very important for studying the oxidation mechanism of these films since oxygen can diffuse through the voids present in between the columns and grain boundaries. Hones *et al.*²¹ have shown that in the case of the binary TiN system the morphology of the coatings significantly influences the oxidation rate and films with a pronounced columnar morphology oxidise seven times faster than those with a dense and fine grained morphology.

The precise nature of the coating microstructure depends on the mobility of deposited adatoms which in turn can be influenced by the deposition temperature, chamber pressure, interlayer and the deposition parameters such as the substrate bias.²² In general PVD films deposited without an interlayer show an open columnar structure of zone 1 type according to the structure model of Thornton.²³ Such films have a relatively low hardness and poor wear resistance²⁴ and do not support any thermal contributions to the overall residual stress, because of the possibility of relaxation of the column boundaries into the intercolumnar spaces perpendicular to the substrate surface.

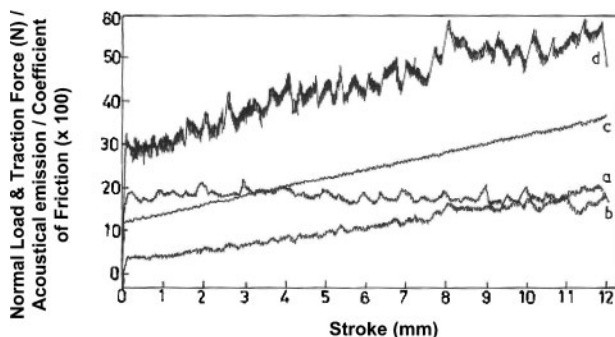
Mechanical properties

An interlayer (like nickel) between the TiN coating and the substrate appears to be beneficial for adhesion owing to chemical interaction and mechanical effects.²⁵ Such an interlayer is expected to be hardened by the presence of oxygen, carbon and nitrogen in solid solution. In addition, the interlayer may act as a compliant region and relax the shear stress at the interface.²⁶ The Ni interlayer reacts with nitrogen during sputtering as the substrate temperature is increased.

However, the effect a soft layer under the coating, results in a decrease in the surface hardness as the load is raised. Thus, a harder interlayer, which can support the integrity, may be expected to eliminate the effect of the substrate and to enhance the surface hardness.

The microhardness values of TiN/MS and TiN/brush plated Ni interlayer samples were measured with an average of minimum three readings taken at each load. The increase in hardness was observed with the decrease in load²⁷ as shown in Table 3.

With the incorporation of brush plated Ni interlayer of $\sim 5.0 \mu\text{m}$ thick, the microhardness of TiN/Ni/MS is found to increase to 2380 HV for a load of 10 g which may be due to the load support provided by the Ni interlayer.



a normal load; b traction force; c acoustic emission; d coefficient of friction

4 Scratch test results for TiN on MS

When a normal load is applied on the film, it introduces a shear stress at the interface between the substrate and the film which, in turn, causes the film to come off. These are two main factors causing the peeling off. One is that the Fe substrate is rather soft, and another is due to the poor adhesion between the TiN coating and Fe substrate (MS). The improvement in the hardness when the Ni interlayer is introduced into TiN on MS can be attributed to the fact that the TiN coating has good adhesion because of its compatibility in thermal expansion coefficient with Ni layer. Thus the employment of brush plated Ni interlayer in the TiN coating on the MS substrate, i.e. the TiN/Ni/MS configuration, provides a potential benefit in the hardness of the coating assembly.

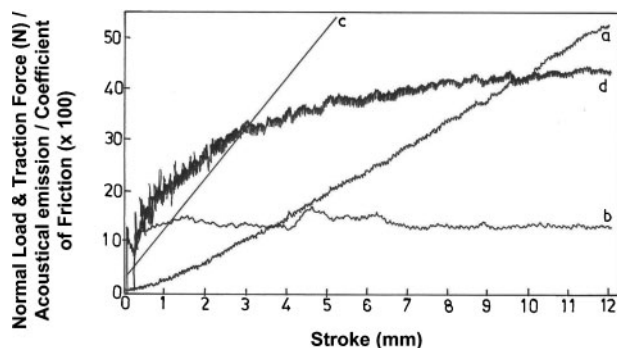
It is reported in the literature that the electroless Ni-P interlayer between TiN and MS substrate has improved the surface hardness by about three times as high.²⁶

The results of scratch tests, which were conducted to determine the adhesion of the hard coating to the substrate, are shown in Fig. 4. A change in the traction force curve was observed for TiN/MS specimen at 4 mm stroke length, which may be due to mild plastic deformation in the coatings. The cohesive failure, i.e. failure within the coating, occurs at 20 N critical load. An appreciable change in the traction curve at 8 mm stroke length and the corresponding change in the coefficient curve were observed. In addition, acoustic emission curve also significantly changes with respect to the coefficient of friction, which may be due to adhesive failure between the coating/substrate interfaces. The coated layer was found to peel off at a critical load of 28 N whereas for the TiN/Ni/MS stack, the cohesive failure was observed at 43 N as shown in Fig. 5. An appreciable change in the traction force curve was observed at 9.5 mm stroke length and the adhesive failure also occurs. The TiN/Ni/MS stack layer was found to peel off only at the critical load of 98 N.

The tribological characteristics of these films were measured using the block on ring test. The ring material used for this test is high chromium high carbon tool steel (850 HV). Low and smooth friction behaviour typified by a steady trace at an average value of 0.3 friction coefficient was observed for TiN/Ni/MS stack whereas a higher value of 0.5 was

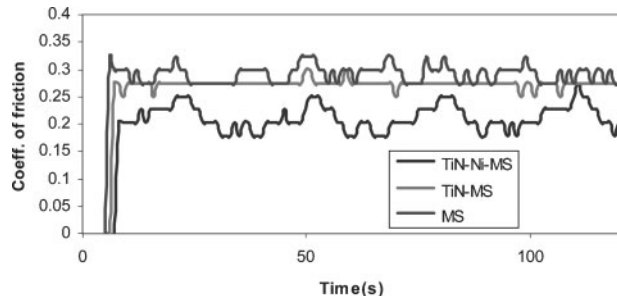
Table 3 Vicker's hardness at different loads for TiN coatings on MS

Sample	50 g	25 g	10 g
TiN (2 μ m)	612	1010	1680
TiN (2 μ m)/Ni (5 μ m)/MS	890	1420	2380

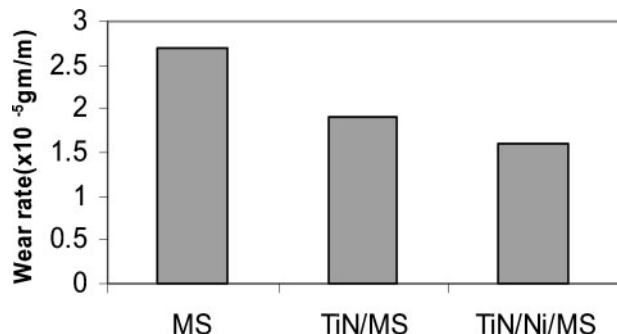


a normal load; b traction force; c acoustic emission; d coefficient of friction

5 Scratch test results for TiN/Ni on MS

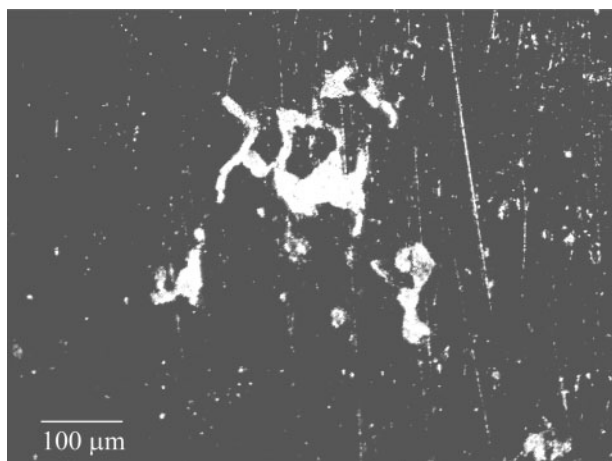


6 Variation of coefficient of friction with time for a MS, b TiN on MS and c TiN/Ni on MS

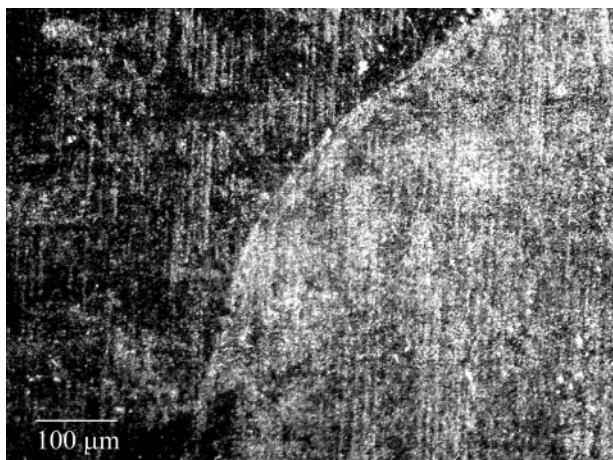


7 Wear rate of steel ring after sliding against MS, TiN/MS and TiN/Ni/MS

observed for the TiN/MS specimen. The lower friction coefficient and wear rate observed in Figs. 6 and 7 respectively for the TiN/Ni/MS stack indicated that the stack has better wear resistance. A sufficiently high hardness of the coated layer and the substrate and the superior adhesion of the layer to the substrate are prerequisite to the excellent wear properties of a coated material.²⁸ The wear tracks that were formed by applying 100 N on the surface of the TiN layer coated on MS and Ni/MS samples are shown in Figs. 8 and 9 respectively. It is seen that the specimen is mainly abrasively worn out coating got peeled off with the MS substrate exposed and plastic deformation of wear debris is clearly shown in the central region of Fig. 8 for the TiN/MS sample. Whereas, TiN coating on Ni/MS substrate did not show any wear debris or peeloff tendency as seen in Fig. 9, but reveals only the wear tracks not showing the substrate unlike the TiN coating on bare MS substrate. Delamination of the coated layer is also visible which can be attributed to the inability of the TiN layer to sustain the same amount of elastoplastic deformation (100 N) of the bare softer MS substrate experienced during the



8 Optical micrograph of TiN on MS sample after wear tests



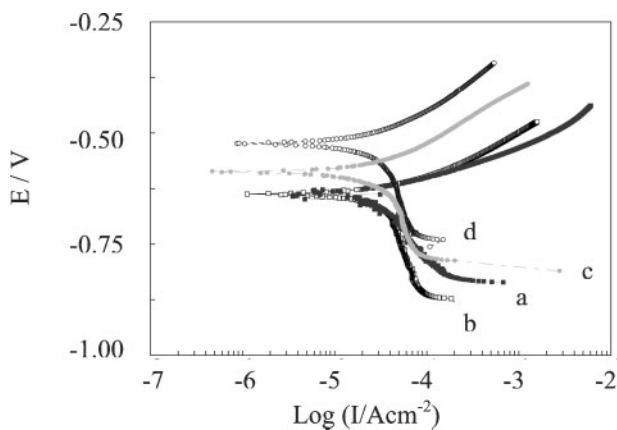
9 Optical micrograph of TiN/Ni on MS sample after wear tests

cyclic loading and unloading process.²⁹ While the wear mechanism of TiN/Ni/MS stack is based on adhesive wear, which results in abrasive particles.

Potentiodynamic polarisation studies

The potentiodynamic polarisation curves obtained for the MS, brush plated Ni, sputtered TiN and TiN/Ni/MS in 3.5% (w/v) NaCl electrolyte are presented in Fig. 10.

The E_{corr} and I_{corr} values have been calculated using the Tafel extrapolation method and are given in Table 4. There is an appreciable increase in corrosion resistance for the TiN/Ni on MS substrate compared to TiN/MS, Ni/MS, and bare MS substrate. E_{corr} and I_{corr} values improve (a less negative value of E_{corr} and lower value of I_{corr} signify an improvement in corrosion) for TiN/Ni on MS substrate. For the TiN/brush plated Ni/MS stack the corrosion current is observed to be the lowest, $0.84 \times 10^{-5} \text{ A cm}^{-2}$, as indicated in Table 4. The corrosion current is as high as $3.31 \times 10^{-5} \text{ A cm}^{-2}$ for the TiN/MS system in which the rapid corrosion of iron takes place at the cavities of the TiN coating owing to the combined effect of the rather noble steady state potential of the TiN



10 Potentiodynamic curves for a bare substrate, b TiN on MS, c Ni on MS and d TiN/Ni/MS

coating and the relatively active iron species. Consequently, the corrosion of MS is accelerated in spite of the TiN coating. However, in the TiN/brush plated Ni/MS stack the brush plated Ni interlayer tends to act as a barrier which effectively retards the corrosion of iron.

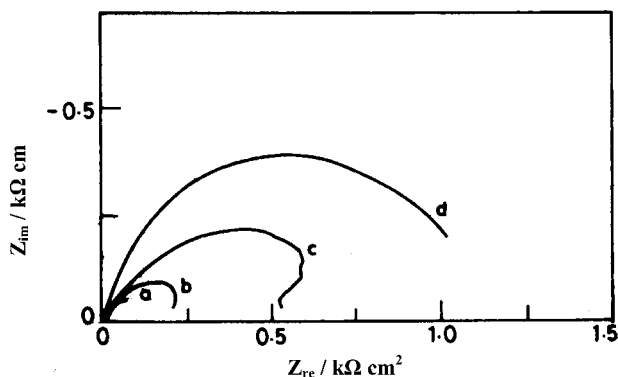
The same three electrode cell stack, as used for the potentiodynamic polarisation experiments, was employed for the AC impedance investigations. Impedance measurements were made at OCP applying an AC signal 10 mV in the frequency range of 10 Hz to 1 MHz. The Nyquist and Bode plots for the samples used for corrosion tests in 3.5% (w/v) NaCl solution are shown in Figs. 11 and 12 respectively.

When the sample is immersed in the electrolyte the defects in the coating provide the direct diffusion path for the corrosive media. In this process the galvanic corrosion cells are formed and the localised corrosion dominates the corrosion process. The proposed equivalent circuit for such a system is shown in Fig. 13. The parameters in the equivalent circuit R_{pore} and C_{coat} are related to the properties of the coating and the electrolyte/coating interface reactions. R_{ct} and C_{dl} are related to the charge-transfer reaction at the electrolyte/substrate interface. The R_{ct} increases (Table 4) in the following order: steel substrate < TiN/substrate < TiN/Ni/substrate which shows that TiN/Ni coating on steel substrate has higher corrosion resistance.

The increase in R_{ct} values and decrease in C_{dl} values for the TiN/brush plated Ni/MS stack confirm the better corrosion resistance of these systems compared to TiN/MS and bare MS substrate. A more semicircular region in the case of the TiN/brush plated Ni/MS stack indicates that this system has maximum corrosion resistance, as observed from the high frequency region of the impedance spectra. The porosity of the nitride metal coatings with brush plated Ni interlayer is found to be lower than that of the coatings without Ni interlayer. The corrosion behaviour of the system is further illustrated by Bode plots in Fig. 12 where it can be seen that the MS has the lowest absolute impedance.

Table 4 Potentiodynamic polarisation data of steel substrate, TiN/MS, TiN/Ni/MS in 3.5%NaCl solution

Sample	E_{corr} versus SCE, mV	b_a , V dec ⁻¹	b_c , V dec ⁻¹	I_{corr} , A cm ⁻²	Corr. rate, mpy	R_{ct} , Ω cm ⁻²	C_{dl} , F cm ⁻²	P , %
MS substrate	-0.651	0.06	-0.16	5.6×10^{-5}	2.5×10^{-5}	62.2	7.7×10^{-3}	-
TiN on MS	-0.649	0.08	-0.55	3.3×10^{-5}	2.0×10^{-5}	193.4	2.0×10^{-4}	2.08×10^{-1}
Ni on MS	-0.568	0.09	-0.49	2.9×10^{-5}	1.2×10^{-5}	675.2	2.5×10^{-4}	4.64×10^{-3}
TiN/Ni/MS	-0.504	0.10	-0.57	0.8×10^{-5}	1.0×10^{-5}	1171.3	2.5×10^{-5}	2.68×10^{-4}

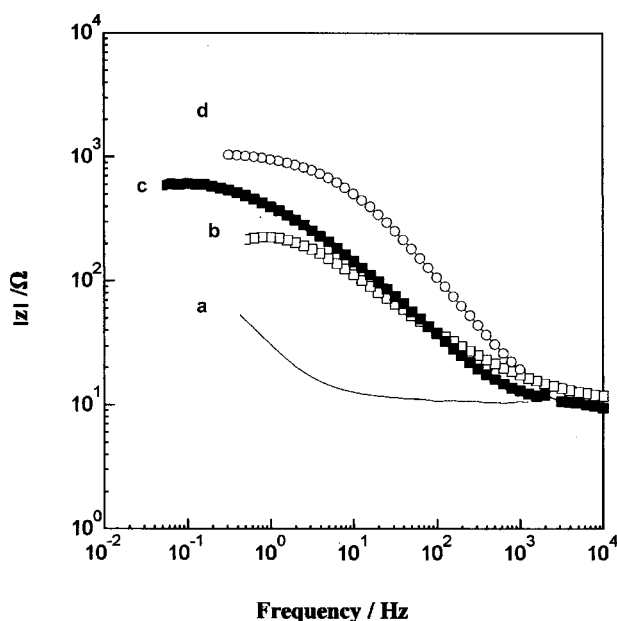


11 Nyquist plot of *a* bare substrate, *b* TiN on MS, *c* Ni on MS and *d* TiN/Ni/MS

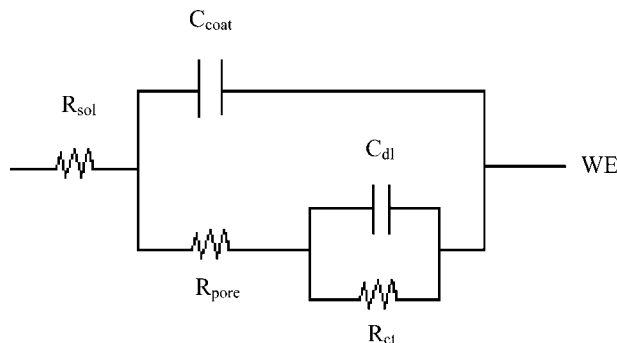
The values of absolute impedance of the alloy system are significantly higher than those of the MS substrate. This again confirms that the TiN/Ni layer on MS provides better corrosion protection to the steel substrate.

Conclusion

In the present study, TiN thin films were successfully deposited on MS and with ~ 5.0 μm thick brush plated Ni interlayer by reactive DC magnetron sputtering technique. These films had preferred orientation along (111) and (200). For TiN with Ni interlayer thin film, texture coefficients of (200) plane are found to increase which shows the improvement in the crystallinity of the layers. TiN films had columnar structure with voids and boundaries and with the Ni interlayer, a denser microstructure was observed. With the incorporation of brush plated Ni interlayer, the microhardness of titanium nitride coatings on MS was found to increase which may be due to the load support provided by the Ni interlayer. The results of wear track investigation and inspection of wear debris showed that TiN is worn by a mainly abrasive wear mechanism, while the wear mechanism of TiN/Ni is based on adhesive wear which results in abrasive particles. The potentiodynamic polarisation and the electrochemical impedance spectroscopy measurements showed that the TiN/Ni/MS stack exhibited better corrosion resistance as



12 Bode plot (Z versus frequency) of *a* bare substrate, *b* TiN on MS, *c* Ni on MS and *d* TiN/Ni/MS



13 Equivalent circuit to fit electrochemical impedance data of TiN on MS

compared to the TiN and Ni films deposited on steel substrate and bare MS substrate.

Acknowledgement

One of the authors (B. Subramanian) thanks the Department of Science and Technology, New Delhi for a research grant under SERC Fast Track scheme no. SR/FTP/CS-23/2005.

References

1. J. Hems: *Semicond. Int.*, 1990, **12**, 100.
2. A. Armigliato, M. Finetti, J. Garrido, S. Guerri, P. Ostojica and A. Scorzoni: *J. Vac. Sci. Technol. A*, 1985, **3A**, 2237.
3. J. M. Wang, W. G. Liu and T. Mei: *Ceram. Int.*, 2004, **30**, 1921.
4. N. D. Cuong, D.-J. Kim, B.-D. Kang, C. S. Kim and S.-G. Yoon: *Microelectron. Reliab.*, 2007, **47**, 752.
5. R. Knitter, W. Bauer, D. Gohring and J. Hauelt: *Adv. Eng. Mater.*, 2001, **3**, 49.
6. O. Sánchez, M. Hernández-Vélez, D. Navas, M. A. Auger, J. L. Baldonado, R. Sanz, K. R. Pirota and M. Vázquez: *Thin Solid Films*, 2006, **495**, 149.
7. Y. Chen, L. T. Chadderton, J. F. Gerald and J. S. Williams: *Appl. Phys. Lett.*, 1999, **74**, 99.
8. S. V. Hainsworth and W. C. Soh: *Surf. Coat. Technol.*, 2003, **163**, 515.
9. H. D. Na, H. S. Parka, D. H. Junga, G. R. Leea, J. H. Joob and J. J. Leena: *Surf. Coat. Technol.*, 2003, **41**, 169.
10. L. Combadiere and J. Machel: *Surf. Coat. Technol.*, 1996, **88**, 17.
11. Y. Li, L. Qu and F. Wang: *Corros. Sci.*, 2003, **45**, 1367.
12. H. C. Barshilia, M. S. Prakash, M. Poojari and K. S. Rajam: *Trans. Inst. Met. Finish.*, 2004, **82**, 123.
13. H. A. Jehn: *Surf. Coat. Technol.*, 2000, **125**, 212.
14. M. Shiao, S. Kao and F. Shieu: *Thin Solid Films*, 2000, **375**, 163.
15. S. B. Hu, J. P. Tu, Z. Mei, Z. Z. Li and X. B. Zhang: *Surf. Coat. Technol.*, 2001, **141**, 174.
16. H. C. Mu, J. Seok and R. Y. Lin: *J. Electrochem. Soc.*, 2003, **150**, c67.
17. S. B. Hu, J. P. Tu, Z. Mei, Z. Z. Li and X. B. Zhang: *Surf. Coat. Technol.*, 2001, **141**, 174.
18. B. Subramanian, S. Mohan, S. Jayakrishnan and M. Jayachandran: *Curr. Appl. Phys.*, 2007, **7**, 305.
19. P. Hones, C. Zakri, P. E. Schmid, F. Lery and O. R. Shojel: *Appl. Phys. Lett.*, 2000, **76**, 3194.
20. J. W. Lim, H. S. Park, T. H. Park, J. J. Lee and J. Joo: *J. Vac. Sci. Technol. A*, 2000, **18A**, 524.
21. P. Hones, C. Zakri, P. E. Schmid, F. Lery and O. R. Shojel: *Appl. Phys. Lett.*, 2000, **76**, 3194.
22. D. S. Rickerby and S. J. Bull: Proc. 16th Leeds-Lyon Symp. on 'Tribology: mechanics of coatings', (ed. D. Dowson et al.), 337; 1990, Amsterdam, Elsevier.
23. J. A. Thornton: *J. Vac. Sci. Technol. A*, 1986, **4A**, 2309.
24. S. J. Bull, D. S. Rickerby, T. Robertson and A. Hendry: *Surf. Coat. Technol.*, 1988, **36**, 743.
25. J. E. Sundgren and H. T. G. Hentzell: *J. Vac. Sci. Technol. A*, 1986, **4A**, (5), 2259.
26. J. G. Duh and J. C. Poong: *Surf. Coat. Technol.*, 1993, **56**, 257.
27. K. Singh, A. K. Grover, M. K. Totlani and A. K. Suri: *Trans. IMF*, 2000, **78**, 23.
28. K. H. Ko, J. H. Ahn, C. S. Bae and H. S. Chung: *Korean J. Mater. Res.*, 1995, **5**, 960.
29. T. S. Jang and S. W. Lee: *Mater. Chem. Phys.*, 1998, **54**, 305.